to cover the behavior of n identical cascaded stages.

Gain dependence on pump power and low frequency (below UHF) noise behavior are expected to be attractive.

References

[1] L. A. Blackwell and K. L. Kotzebe, *Semiconductor Diode Parametric Amplifiers*. Englewood Cliffs, N. J.: Prentice-Hall, 1961.

[2] R. L. Honey, and E. M. T. Jones, "A wide-band UHF travelling wave variable reactance amplifier," *IRE Trans. Microwave Theory Tech*, vol. MTT-8, pp. 351–361, May 1960.

[3] C. V. Bell and G. Wade, "Circuit considerations in travelling-wave parametric amplifiers," *IRE WESCON Conv. Rec*, Pt. 2, pp. 75–82, 1959.

[4] R. S. Engelbrecht, "Non-linear-reactance (parametric) travelling-wave parametric amplifiers for UHF," *Dig. Tech. Papers*, 1959 Solid State Circuit Conf., Philadelphia, PA, Feb. 12, 1959.

[5] "Standards on Receivers, definition of terms 1952," *Proc. IRE*, vol. 40, p. 1681, 1952.

[6] H. A. Haus and R. B. Adler, "Optimum noise performance of linear amplifiers," *Proc. IRE*, vol. 46, pp. 1517–1533, Aug. 1958.

[7] ——, *Circuit theory of Linear Noisy Networks*. New York: Technology and Wiley, 1959.

[8] C. S. Aitchison and A. Wong, "A VHF hybrid parametric amplifier," this issue, pp. 825–832.

High-Accuracy WKB Analyses of α-Power Graded-Core Fibers

KIMIYUKI OYAMADA, STUDENT MEMBER, IEEE, AND TAKANORI OKOSHI, MEMBER, IEEE

Abstract—**The WKB method is an effective approach to the analyses of propagation characteristics of optical fibers. However, conventional WKB analyses can not be applied to close-to-cutoff modes because the effect of core-cladding boundary is not considered exactly.**

This paper proposes two improved WKB analyses which consider the above effect more exactly. Both of these methods are applicable to the close-to-cutoff modes. The first one is superior in accuracy (for example, relative error in cutoff frequencies $\lesssim 10^{-5}$), but applicable only to quadratic profiles. The second one is applicable to general α-power profiles; the accuracy is poorer but tolerable for most practical purposes.

I. Introduction

MANY METHODS have been developed for the analysis of propagation characteristics of optical fibers having arbitrary refractive-index profiles. Among these, the WKB method [1],[2] is relatively simple and comprehensive. However, it is essentially an approximate analysis, and usually gives large error for close-to-cutoff modes.

A significant fact found by the conventional WKB analyses was that the multimode dispersion was minimized for a quasiquadratic (parabolic) profile [1]. It was also found that the maximum delay difference between propagating modes for such a profile was approximately $T\Delta^2/2$, where T and Δ denote the propagation time and the relative refractive-index difference (see (1)), respectively.

However, more exact analyses such as those by Rayleigh–Ritz method [3], finite-element method [4], and power-series expansion method [5] reveal that the delay-time difference between the well-confined and close-to-cutoff modes approaches $T\Delta$. This value is much greater than the above WKB prediction: $T\Delta^2/2$. The principal reason for such an error in the conventional WKB analyses [1],[2] is that the effect of the discontinuity in the slope of the index profile at core-cladding boundary is not taken into account. For the same reason, the effect of the index valley at the core-cladding boundary, which is claimed to be effective for reducing the multimode dispersion [6], cannot be analyzed by the conventional WKB analyses. Recently, Olshansky [7] and Ikuno [8] proposed modified WKB analyses to improve these drawbacks.

This paper proposes two WKB analyses which consider the above effect more exactly. These are applicable either to the close-to-cutoff modes or to the index profiles with valley. The first method is somewhat similar to the Olshansky's, but the accuracy is improved. The relative error in the cutoff frequencies of LP_{ml} modes in quadratic-profile fibers is below 10^{-5} for most modes. However, this method is difficult to apply to index profiles other than the quadratic one. The second method uses an asymptotic solution different from the first, and is applicable to general α-power profiles; however, the accuracy is poorer.

II. WKB Formulations

The index profile is assumed to be expressed as

$$n(r) = n_1\left[1 - 2\Delta f(r)\right]^{1/2} \tag{1}$$

where r denotes the radial coordinate normalized by the core radius a, and $f(r)$ is a function given as

$$f(r) = \begin{cases} r^\alpha, & r \leqslant 1 \quad (2) \\ 1, & r > 1. \quad (3) \end{cases}$$

In this case, the scalar wave equation [9] can be written as

$$\frac{1}{r}\frac{d}{dr}\left(r\frac{dR}{dr}\right) + \left\{u^2 - v^2 f(r) - \frac{m^2}{r^2}\right\} R = 0 \tag{4}$$

where $R(r)$ is the function representing the field distribution

Manuscript received January 7, 1980; revised March 18, 1980.

The authors are with the Department of Electrical Engineering, University of Tokyo, Bunkyo-ku, Tokyo 113, Japan.

0018-9480/80/0800-00839$00.75 ©1980 IEEE

TABLE I
SOLUTIONS OF THE FIELD FUNCTION $R(r)$, METHOD R IS THE CONVENTIONAL WKB METHOD (METHOD O IS OLSHANSKY'S ANALYSIS [7], METHODS A AND B ARE THOSE PROPOSED IN THIS PAPER. SYMBOL DENOTES "NOT CLOSE TO")

	(i) $0 \lesssim r \lesssim r_1$	(ii) $r \cong r_1$	(iii) $r_1 \lesssim r \lesssim r_2$	(iv) $r \cong r_2$	(v) $r_2 \lesssim r \leq 1$	(vi) $1 \leq r$
R	$(rp)^{-\frac{1}{2}}\exp(-\psi_1)$	$(rp)^{-\frac{1}{2}}\Psi^{(1)}(\psi_1)$	$2\lvert rp\rvert^{-\frac{1}{2}}\cos(\lvert\psi_1\rvert-\frac{\pi}{4})$	$(rp)^{-\frac{1}{2}}[\sin\theta\Psi^{(1)}(\psi_2)$ $+\sqrt{3}\cos\theta\Psi^{(2)}(\psi_2)]$	$(rp)^{-\frac{1}{2}}\exp(-\psi_2)$	
A	← same as above →				$(rp)^{-\frac{1}{2}}[\sin\theta\Psi^{(1)}(\psi_2)$ $+\sqrt{3}\cos\theta\Psi^{(2)}(\psi_2)]$	$(rp)^{-\frac{1}{2}}\exp(-\psi_2)$
O	← same as above →				$(rp)^{-\frac{1}{2}}[\sin\theta\exp(-\psi_2)$ $+\sqrt{3}\cos\theta\exp(\psi_2)]$	$(rp)^{-\frac{1}{2}}\exp(-\psi_2)$

	(vii) $0 \leq r \lesssim r_3$	(viii) $0 \lesssim r \leq 1$	(ix) $1 \leq r$
B	$(\frac{\pi\phi_1}{2r\lvert g\rvert})^{\frac{1}{2}}J_m(\phi_1)$	$(rg)^{-\frac{1}{2}}[\sin(\Theta-\frac{m}{2}\pi)\Psi^{(1)}(\phi_2)$ $+\sqrt{3}\cos(\Theta-\frac{m}{2}\pi)\Psi^{(2)}(\phi_2)]$	$K_m(wr)$

$$v^2 = a^2k^2n_1^2(2\Delta): \text{normalized frequency} \tag{5}$$

$$u^2 = a^2(n_1^2k^2 - \beta^2) \tag{6}$$

m is the rotational mode number, k and β denote the propagation constants in free space and in the fiber along its axis, respectively.

The approximate solution for $R(r)$ by the conventional WKB method [2], [10] is given as

$$R(r) = (rp)^{-1/2}\exp\left[\pm\int p\,dr\right] \tag{7}$$

where

$$p^2(r) = -\{u^2 - v^2f(r) - m^2/r^2\}. \tag{8}$$

Fig. 1 shows a schematic drawing of the function $p^2(r)$ for an α-power profile. As shown in this figure, $p^2(r)$ has two "turning points" r_1 and r_2 [2], in the vicinities of which the approximation of (7) becomes very poor. In such regions, better solutions are [10]

$$R(r) = \left(\frac{\pi\psi_i}{2rp}\right)^{1/2} I_{\pm 1/3}(\psi_i), \qquad i = 1,2 \tag{9}$$

where

$$\psi_1 = \int_r^{r_1} p\,dr \tag{10}$$

$$\psi_2 = \int_{r_2}^{r} p\,dr \tag{11}$$

and are used for the regions $r \cong r_1$ or $r \cong r_2$, respectively, and I_ν is the νth-order modified Bessel function of the first kind.

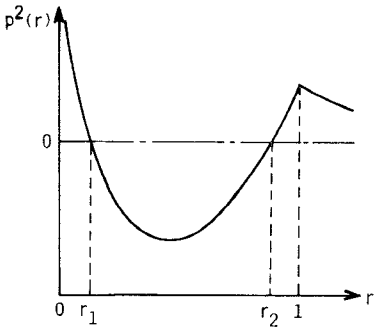

Fig. 1. A schematic drawing of function $p^2(r)$.

By using (7) and (9), the field function $R(r)$ can be approximated in three ways, which are tabulated as methods R, A and O in Table I.

Method R (Reference) denotes the conventional WKB analysis [2], which is shown for comparison. Method A is the first of the two methods proposed in this paper. The only difference between methods R and A is found in the solutions in the region $r_2 \lesssim r \leq 1$, where symbol $\lesssim$ denotes "not close to." Method O denotes Olshansky's analysis [7]; this is discussed in detail in the final part of Section III.

In Table I, $\Psi^{(1)}$ and $\Psi^{(2)}$ used in method R (and also in A and B) are functions defined as

$$\Psi^{(i)}(z) = -\left(\frac{2\pi z}{3}\right)^{1/2}\left[-I_{-1/3}(z) \pm I_{1/3}(z)\right], \qquad i = 1,2 \tag{12}$$

where the double sign is plus for $i=1$ and minus for $i=2$, and

$$\theta=\int_{r_1}^{r_2}|p|dr. \tag{13}$$

In [2], which describes method R in more detail than [1], Petermann gives the solutions near the turning points in terms of Airy functions Ai and Bi instead of $\Psi^{(1)}$ and $\Psi^{(2)}$. However, the identity of his solutions with those in Table I can readily be shown.[1]

In method R, a single formula expresses the solution in the region $r_2 \lesssim r \leqslant 1$ and that in the cladding. However, such a WKB solution gives a good approximation for the field function only when the following condition holds [2]:

$$\left|\frac{Q''}{4Q}-\frac{5}{16}\left(\frac{Q'}{Q}\right)^2\right|\ll Q \tag{14}$$

where $Q=(rp)^2$ and a prime denotes a differentation with respect to $w=\log r$. The above inequality suggests that the approximation is very poor at $r=1$ where the slope of the function $p^2(r)$ changes abruptly (see Fig. 1) and hence Q'' is very large. Thus the conventional WKB solution (method R) gives a large error especially at frequencies close to cutoff where the effect of the above poor approximation is enhanced. In method A, this problem is solved by using two different solutions in regions (v) and (vi). As described later, these two solutions can be joined smoothly at $r=1$ to obtain a proper equation. Method A is applicable even to index profiles having an index step or valley at $r=1$.

Method B in Table I is the second method proposed in this paper; this is based upon a somewhat different idea proposed originally by Kurtz and Streifer [12]. In this method, we first write the asymptotic solution in most of the core as [12]

$$R(r)=\left(\frac{\pi\phi_1}{2r|g|}\right)^2 J_m(\phi_1) \tag{15}$$

where

$$\phi_1=\int_0^r|g|dr \tag{16}$$

$$g^2(r)=-\{u^2-v^2f(r)\}. \tag{17}$$

A schematic drawing of function $g^2(r)$ is shown in Fig. 2. This function becomes zero at $r=r_3$, that is, a little inside the core-cladding boundary. Thus (15) gives a large error near $r=r_3$. To overcome this difficulty, we use another approximate formula in this region

$$R(r)=\left(\frac{\pi\phi_2}{2rg}\right)^{1/2} I_{\pm 1/3}(\phi_2) \tag{18}$$

where

$$\phi_2=\int_{r_3}^r g\,dr. \tag{19}$$

Equation (18) is obtained by assuming $|u^2-v^2f(r)|\gg m^2/r^2$ in (8) and (9).

From (15) and (18), we obtain the solutions B in Table I, where $\Psi^{(1)}$ and $\Psi^{(2)}$ are equal to those defined in (12), and

$$\Theta=\int_0^{r_3}|g|dr. \tag{20}$$

Using method B, we can deal with general α-power profiles (where α is not necessarily an integer) even having an index valley or step at the core-cladding boundary. This is because integrals in (19),(20) can be computed analytically for such general profiles as described in the following.

We assume the index profile as

$$f(r)=\begin{cases}\rho r^\alpha, & 0\leqslant r<1\\ 1, & 1<r\end{cases} \tag{21}$$

where ρ expresses the depth of the index valley (when $\rho>1$) or height of the index step (when $\rho<1$) at the core-cladding boundary. Parameter Θ defined by (20) can be computed, from (17) exactly as

$$\Theta=\frac{u}{v}\left(\frac{u^2}{\rho v^2}\right)^{1/\alpha}B\left(\frac{1}{\alpha},\frac{3}{2}\right) \tag{22}$$

where B denotes a Beta function. The value of ϕ_2 at $r=1$ (which is needed to compute (34) and (35) to appear later) is given approximately as (see Appendix)

$$\phi_{2,r=1}=\alpha^{1/2}u\left(\frac{u}{\rho v}\right)^{1/\alpha}\left[\frac{(\alpha-1)z+1}{2(\alpha-1)}\sqrt{\frac{\alpha-1}{2}z^2+z}\right.$$
$$-\frac{1}{\sqrt{2}\,(\alpha-1)^{3/2}}\log\left|(\alpha-1)z+1\right.$$
$$\left.\left.+\sqrt{2(\alpha-1)}\sqrt{\frac{\alpha-1}{2}z^2+z}\,\right|\right]_{z=(\rho v/u)^{1/\alpha-1}} \tag{23}$$

provided that we can assume that

$$r_3\cong 1 \tag{24}$$

or

$$\alpha\cong 2. \tag{25}$$

III. Proper Equations

Now four sets of solutions for the field function $R(r)$ are given. The proper equations can be derived from each set of these solutions. First, in method R, the proper equation is derived from the condition that the asymptotic form of the solution in region (iv) must coincide with the solutions in regions (v) and (vi). This leads to

$$\cot\theta=0 \tag{26}$$

which gives a quantized condition to the value of θ [2].

[1] As to the relation between Ai, Bi, and $I_{\pm 1/3}$ see, for example, [11, p. 447, equations (10.4.14) and (10.4.18)].

To derive solutions in regions (ii), (iii), and (iv) in Table I, we must consider smooth connections between those in regions (i)–(v), when either Ai and Bi or $\Psi^{(1)}$ and $\Psi^{(2)}$ are used. Such calculation is somewhat lengthy and so far has not been described in detail anywhere. If necessary, refer to [13] to be published.

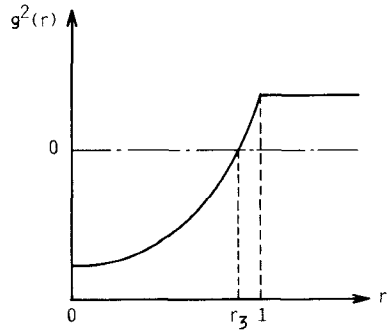

Fig. 2. A schematic drawing of function $g^2(r)$.

In methods A and B, we use the condition that the logarithmic derivatives of the field solutions must be continuous at the core-cladding boundary; that is [3]

$$\lim_{r\to 1-0}\frac{1}{R}\frac{dR}{dr}=\lim_{r\to 1+0}\frac{1}{R}\frac{dR}{dr}. \tag{27}$$

This condition follows from the fact that both $R(r)$ and $dR(r)/dr$ must be continuous at $r=1$. From this condition, the proper equation for method A is given as

$$\cot\theta=\delta \tag{28}$$

where

$$\delta=\frac{1}{\sqrt{3}}\cdot\left[\frac{\gamma[I_{1/3}(\psi_2)-I_{-1/3}(\psi_2)]-p^-[I'_{1/3}(\psi_2)-I'_{-1/3}(\psi_2)]}{\gamma[I_{1/3}(\psi_2)+I_{-1/3}(\psi_2)]-p^-[I'_{1/3}(\psi_2)+I'_{-1/3}(\psi_2)]}\right]_{r=1} \tag{29}$$

$$\gamma=-\frac{1}{2}\left(\frac{p_r^+}{p^+}+2p^++\frac{p^-}{\psi_2}-\frac{p_r^-}{p^-}\right) \tag{30}$$

$$p^{\pm}=\lim_{r\to 1\pm 0}p \tag{31}$$

$$p_r^{\pm}=\lim_{r\to 1\pm 0}\frac{dp}{dr} \tag{32}$$

a prime denotes a differentiation with respect to the argument, and suffix r denotes a differentiation with respect to r. Similarly, the proper equation for method B is given as

$$\cot\left(\Theta-\frac{m}{2}\pi\right)=\delta' \tag{33}$$

where m is the rotational mode number,

$$\delta'=\frac{1}{\sqrt{3}}\cdot\left[\frac{\Gamma[I_{1/3}(\phi_2)-I_{-1/3}(\phi_2)]-g^-[I'_{1/3}(\phi_2)-I'_{-1/3}(\phi_2)]}{\Gamma[I_{1/3}(\phi_2)+I_{-1/3}(\phi_2)]-g^-[I'_{1/3}(\phi_2)+I'_{-1/3}(\phi_2)]}\right]_{r=1} \tag{34}$$

$$\Gamma=-\left[\frac{wK_{m-1}(w)}{K_m(w)}\right]-\frac{1}{2}\left(\frac{g^-}{\phi_2}-\frac{g_r^-}{g^-}-1\right) \tag{35}$$

$$w^2=v^2-u^2 \tag{36}$$

$$g^-=\lim_{r\to 1-0}g \tag{37}$$

$$g_r^-=\lim_{r\to 1-0}\frac{dg}{dr} \tag{38}$$

and K_m denotes mth-order modified Bessel function of the second kind.

The above proper equations (26), (28), and (33) have similar forms. The only difference between (26) and (28) is found in the right-hand sides. For well-confined modes, ψ_2 is very large. This makes δ very small (29). Thus (28) can be approximated as (26). For close-to-cutoff modes, however, δ cannot be neglected, and (26) and (28) give much different results. Thus the conventional WKB analysis [1],[2] gives a large error for close-to-cutoff modes.

Olshansky's analysis (method O in Table I) is similar to method A. However, in region (v), he used an asymptotic form of the solution used in method A and consequently obtained a simpler proper equation [7]

$$\cot\theta=\delta_0=-\frac{1}{2}\frac{p^+p_r^--p^-p_r^++2p^-p^+(p^--p^+)}{p^+p_r^--p^-p_r^++2p^-p^+(p^-+p^+)}e^{-2\phi_2(1)} \tag{39}$$

instead of (28). However, the above asymptotic form generates a large error in the vicinity of the turning point r_2. Therefore, when the turning point r_2 approaches the core-cladding boundary, in other words at near-cutoff frequencies, Olshansky's analysis gives a relatively large error as shown in Section V.

When $m=0$, that is, for LP_{0l} modes, $p^2(r)=g^2(r)$ and the inner turning point r_1 disappears. Therefore, methods R, A, and O, which assume the presence of that turning point, cannot be applied to LP_{0l} modes as they stand.[2] Method B is applicable also to such modes.

IV. Delay Time

The delay time per unit distance is given as

$$t=\frac{1}{c}\frac{d\beta}{dk} \tag{40}$$

where c denotes the velocity of light. We compute first the delay time using method A. Making the derivatives of both sides of (28) with respect to k, we obtain

$$-(1+\delta^2)\left(\frac{\partial\theta}{\partial k}+\frac{\partial\theta}{\partial\beta}\frac{d\beta}{dk}\right)=\frac{\partial\delta}{\partial k}+\frac{\partial\delta}{\partial\beta}\frac{d\beta}{dk}. \tag{41}$$

Hence the delay time per unit length is given as

$$t=-\frac{1}{c}\left(\frac{\partial\theta/\partial k}{\partial\theta/\partial\beta}\right)\left[\frac{(1+\delta^2)+(\partial\delta/\partial k)/(\partial\theta/\partial k)}{(1+\delta^2)+(\partial\delta/\partial\beta)/(\partial\theta/\partial\beta)}\right]. \tag{42}$$

If we start from (26), we can simply let $\delta=0$ in the above equations. In this case, the factor in the bracket in (42) becomes unity. This fact suggests that this factor gives a correction to the conventional WKB analysis [7]. In case of method B, parameters in (42) should simply be replaced as

$$\delta\to\delta' \tag{43}$$

$$\theta\to\left(\Theta-\frac{m}{2}\pi\right). \tag{44}$$

[2]Some corrections of the formulations might enable us to deal with the LP_{0l} modes using these methods.

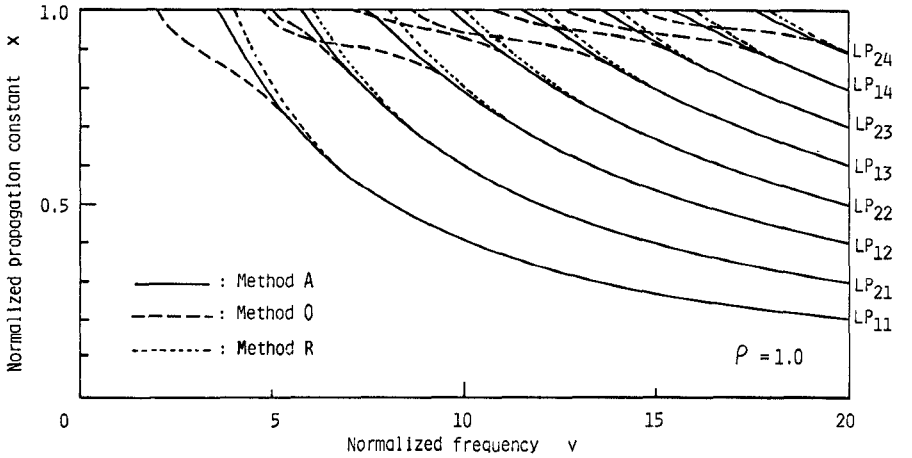

Fig. 3. Normalized propagation constant for the quadratic profile computed by methods A, O, and R.

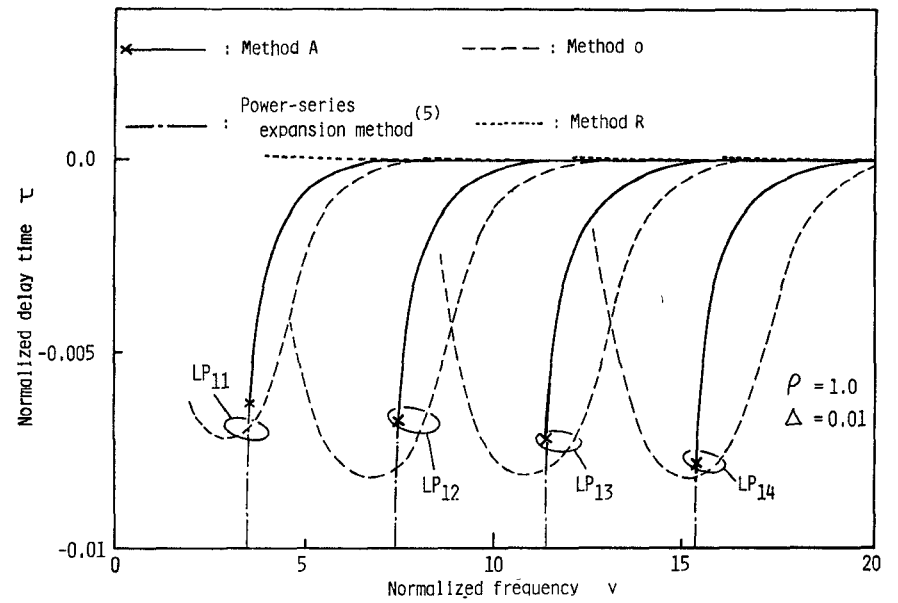

Fig. 4. Normalized delay time for the quadratic profile computed by methods A, O, R and the series-expansion method [5].

V. Numerical Calculations

The propagation characteristics can be calculated numerically by using the proper equations and delay-time formulas.

In method A, the proper equation (28) can be solved without much difficulty only for the quadratic ($\alpha=2$) profile. It is because the integrals in (11) and (13) can hardly be computed analytically for cases $\alpha\neq 2$ (see (8)); for such cases numerical calculation is required.

The propagation constant and delay time for the quadratic profile obtained by method A are shown by solid curves in Figs. 3 and 4, respectively, where β and t are expressed by normalized variables defined as[3]

$$x=\frac{k^2n_1^2-\beta^2}{k^2n_1^2(2\Delta)} \tag{45}$$

$$\tau=\frac{ct}{n_1}-1. \tag{46}$$

The dotted curves and broken curves in Figs. 3 and 4 show the results of the conventional WKB analysis (method R) and those of Olshansky's analysis [7], respectively.

The results of computation by method A show fairly good agreement with more rigorous analyses by finite-element and power-series expansion methods [5] shown by dash-dotted curves; the difference can hardly be shown on the graphs. A relatively large error is found only in the delay-time characteristics at near-cutoff frequencies. The relative error in the cutoff frequencies for LP_{ml} modes is shown Fig. 5; the error is less than 10^{-5} for those modes for which $l>4$.

The propagation constant and delay time computed by using method B are shown in Figs. 6 and 7, respectively, for $\alpha=2$, 4, 10, and $\rho=1$. Table II shows the normalized frequencies giving $x=0.5$ and 0.9 in the dispersion char-

[3]A variable defined as $b=1-x$ is also used in many papers. See, for example [14].

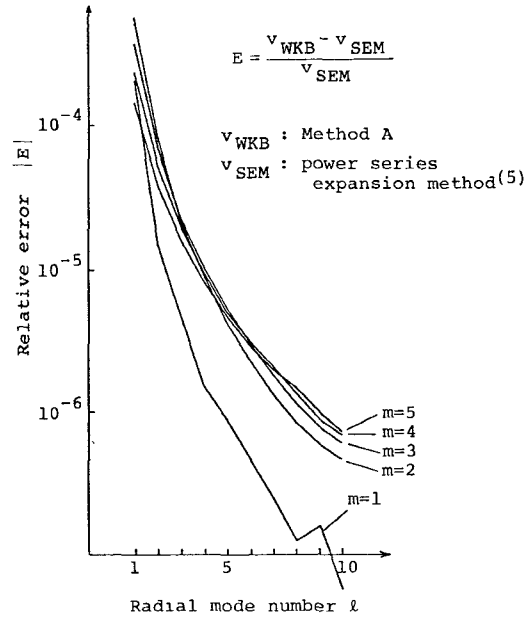

Fig. 5. Error in the normalized cutoff frequencies of LP_{ml} modes for the quadratic profile computed by method A. The rigorous values V_{SEM} have been obtained by power-series expansion method.

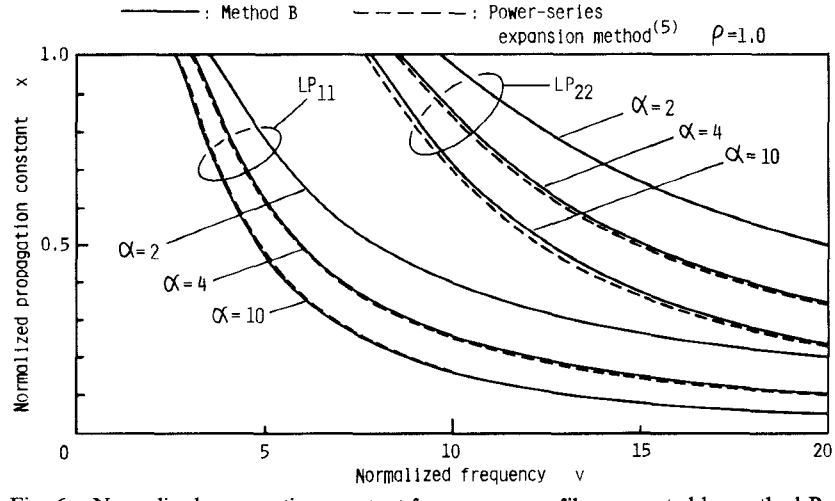

Fig. 6. Normalized propagation constant for α-power profiles computed by method B.

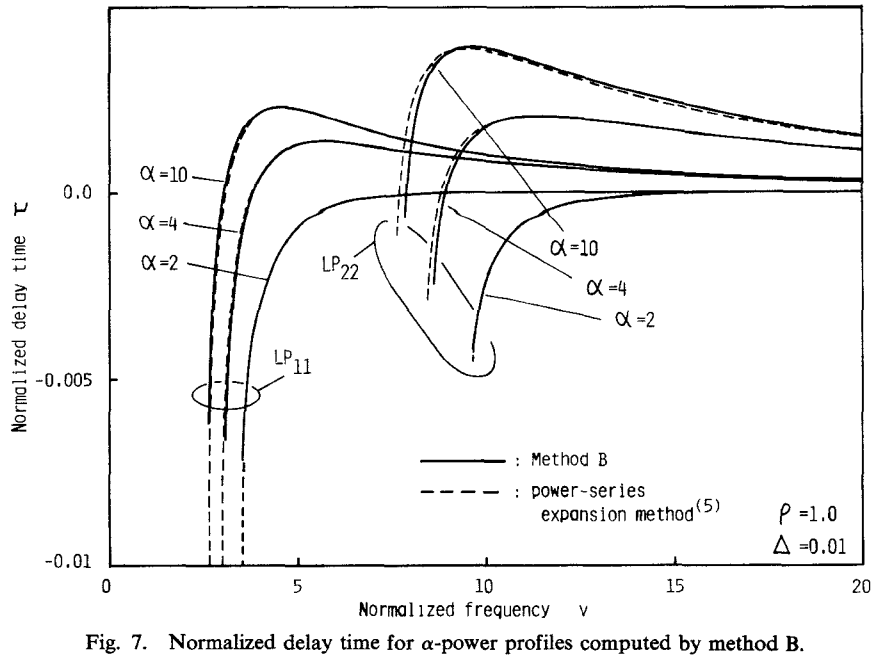

Fig. 7. Normalized delay time for α-power profiles computed by method B.

TABLE II
NORMALIZED FREQUENCIES GIVING $x=0.5$ AND 0.9, AND THE CORRESPONDING ERRORS (IN THE PARENTHESES) IN METHOD B

mode	LP_{11}-mode		LP_{22}-mode	
x	0.9	0.5	0.9	0.5
$\alpha = 2$	4.2200 (-0.0005)	7.99026 (-0.00007)	10.9989 (0.0002)	19.9999 (-0.00001)
$\alpha = 4$	3.57147 (0.0195)	5.98259 (0.0158)	9.54145 (0.0156)	15.1050 (0.0152)
$\alpha = 10$	3.02957 (-0.0072)	4.81216 (-0.0086)	8.56071 (0.0219)	12.5471 (0.0205)

acteristics, and the error obtained by comparing those with more rigorous data [5]. In Figs. 6 and 7, a relatively large error is found again in the delay-time near cutoff. In other parts the accuracy is practically satisfactory. The quadratic profile ($\alpha=2$) gives the minimum error because (23) is exact for this profile.

VI. CONCLUSION

Two improved WKB analyses of α-power fibers have been proposed. The first one is a modification of the conventional WKB method; this can be applied also to close-to-cutoff modes, to which the conventional ones are not applicable. The accuracy is excellent for most of the propagating modes (see Fig. 5). However, this method can hardly be applied to those profiles in which $\alpha \neq 2$.

The second one is applicable to general α-power profiles. The error is relatively large, but is tolerable in practical applications (see Figs. 5, 6, and 7, and Table II).

APPENDIX
DERIVATION OF (23)

$$\phi_{2,r=1} = \int_{r_3}^{1} \sqrt{\rho v^2 r^\alpha - u^2}\, dr$$

$$= u\left(\frac{u^2}{\rho v^2}\right)^{\alpha} \int_0^{r_3^{-1}-1} \sqrt{(1+z)^\alpha - 1}\, dz. \quad \text{(A.1)}$$

The integrand can be approximated as

$$\sqrt{(1+z)^\alpha - 1} = \left[\alpha z + \frac{\alpha(\alpha-1)}{2} z^2 + \frac{\alpha(\alpha-1)(\alpha-2)}{6} z^3 + \cdots\right]^{1/2}$$

$$\cong \left[\alpha z + \frac{\alpha(\alpha-1)}{2} z^2\right]^{1/2} \quad \text{(A.2)}$$

provided that

$$r_3 \cong 1 \quad \text{(A.3)}$$

or

$$\alpha \cong 2. \quad \text{(A.4)}$$

We can compute the integral of (A.2) analytically.

REFERENCES

[1] D. Gloge and E. A. Marcatili, "Multimode theory of graded-core fibers," *Bell Syst. Tech. J.*, vol. 52, no. 9, pp. 1563–1578, Nov. 1973.

[2] K. Petermann, "The mode attenuation in general graded core multimode fibers," A.E.U., vol. 29, no. 7/8, pp. 345–348, 1975.

[3] T. Okoshi and K. Okamoto, "Analysis of wave propagation in inhomogeneous optical fibers using a variational method," *IEEE Trans. Microwave Theory Tech.*, vol. MTT-22, pp. 938–945, Nov. 1974.

[4] K. Okamoto and T. Okoshi, "Vectorial wave analysis of inhomogeneous optical fibers using finite element method," *IEEE Trans. Microwave Theory Tech.*, vol. MTT-26, pp. 109–114, Feb. 1978.

[5] K. Oyamada and T. Okoshi, "High-accuracy numerical data on propagation characteristics of α-power graded-core fibers," *IEEE Trans. Microwave Theory Tech.*, to be published.

[6] K. Okamoto and T. Okoshi, "Computer-aided synthesis of the optimum refractive-index profile for a multimode fiber," *IEEE Trans. Microwave Theory Tech.*, vol. MTT-25, pp. 213–221, Mar. 1977.

[7] R. Olshansky, "Effect of the cladding on pulse broading in graded-index optical waveguides," *Appl. Opt.*, vol. 16, no. 8, pp. 2171–2174, Aug. 1977.

[8] H. Ikuno, "Analysis of wave propagation in inhomogeneous dielectric slab waveguides," *IEEE Trans. Microwave Theory Tech.*, vol. MTT-26, pp. 261–266, Apr. 1978.

[9] S. Kawakami and J. Nishizawa, "An optical waveguide with the optimum distribution of the refractive index with reference to waveform distortion," *IEEE Trans. Microwave Theory Tech.*, vol. MTT-16, pp. 814–818, Oct. 1968 (see equation (34)).

[10] L. I. Schiff, *Quantum Mechanics*. New York: McGraw-Hill, 1955.

[11] M. Abramowitz and J. A. Stegun, *Handbook of Mathematical Functions*. New York: Dover, 1965.

[12] S. Streifer and C. N. Krutz, "Scalar analysis of radially inhomogeneous guiding media," *J. Opt. Soc. Amer.*, vol. 57, no. 6, pp. 779–786, June 1967.

[13] T. Okoshi, *Optical Fibers*. New York: Academic Press, to be published, Appendix 5A.4.

[14] D. Gloge, "Weakly guiding fibers," *Appl. Opt.*, vol. 10, no. 10, pp. 2252–2258, Oct. 1971.